

PERFORMANCE OF CIRCULAR ANNULAR DIFFUSERS IN INCOMPRESSIBLE FLOW

CONTENTS

	Page
1. NOTATION, UNITS AND DEFINITIONS	1
2. SUMMARY OF DATA PRESENTED AND APPLICABILITY	3
3. FLOW CONDITIONS	4
4. STATIC PRESSURE RECOVERY	4
4.1 Diffusers without Tailpipes	4
4.2 Diffusers with Tailpipes	5
4.3 Some Factors Influencing Pressure Recovery	5
4.3.1 Inlet flow conditions	5
4.3.2 Inlet Reynolds number and Mach number	6
4.3.3 Junction with inlet duct	7
4.3.4 Adjacent components	7
4.3.5 Centre-body supporting struts	7
5. TOTAL-PRESSURE LOSS	7
5.1 Diffusers without Tailpipes	8
5.2 Diffusers with Tailpipes	8
6. EXAMPLE	9
7. DERIVATION	11
8. TABLES	12
FIGURES	13 to 27

PERFORMANCE OF CIRCULAR ANNULAR DIFFUSERS IN INCOMPRESSIBLE FLOW

1. NOTATION, UNITS AND DEFINITIONS

Notation and Units

Three coherent systems of units are given below.

		<i>SI</i>	<i>British</i>	
A	cross-sectional flow area of duct	m ²	ft ²	ft ²
C_{pr}	static-pressure recovery coefficient (see Equation (1.1))	—	—	—
C_{pr}^*	value of C_{pr} attained in a diffuser of optimum area ratio for given length ratio and wall angles	—	—	—
C_{pr}^{**}	value of C_{pr} attained in a diffuser of optimum length ratio for given area ratio and wall angles	—	—	—
D	duct diameter	m	ft	ft
D_h	duct hydraulic or equivalent diameter, $4A/\text{wetted perimeter}$ ($= 2h$ for annulus)	m	ft	ft
h	annulus width, $R_o - R_i$ (see Sketch 1.1)	m	ft	ft
K_t	total-pressure loss coefficient (see Equation (1.2))	—	—	—
L	axial length of diffuser (see Sketch 1.1)	m	ft	ft
L_d	length of parallel duct downstream of diffuser (tailpipe) (see Sketch 1.1)	m	ft	ft
L_u	length of parallel duct upstream of diffuser (see Sketch 1.1)	m	ft	ft
m	mass flow rate	kg/s	lb/s	slug/s
p	static pressure	*N/m ²	pdl/ft ²	lbf/ft ²
p_t	total pressure (see Equation (1.3))	*N/m ²	pdl/ft ²	lbf/ft ²
R	duct radius	m	ft	ft
Re	inlet Reynolds number, $\bar{V}_1 h_1 / \nu_1$	—	—	—
r	annulus radius ratio, R_i / R_o	—	—	—

For footnotes see end of Notation Section.

V	local axial flow velocity	m/s	ft/s	ft/s
\bar{V}	area-averaged flow velocity, $m/\rho A$	m/s	ft/s	ft/s
α	kinetic energy coefficient, $[1/(\bar{V}^3 A)] \int_A V^3 dA$	—	—	—
ν	fluid kinematic viscosity	m ² /s	ft ² /s	ft ² /s
ρ	fluid density	kg/m ³	lb/ft ³	slug/ft ³
ϕ	angle between duct wall and duct axis (positive for a diverging cone)	degrees	degrees	degrees

* Use of the name Pascal (Pa) for this unit is now recommended in the SI system.

Suffixes

e	refers to conditions at exit from diffuser or diffuser-tailpipe combination
i	refers to inner wall of annulus
o	refers to outer wall of annulus
1	refers to conditions at diffuser entry
2	refers to conditions at diffuser exit
3	refers to conditions at tailpipe reference point, $4h_2$ from diffuser exit

Definitions

The static-pressure recovery coefficient is defined by

$$C_{pr} = \frac{p_e - p_1}{\frac{1}{2}\rho \bar{V}_1^2}, \quad (1.1)$$

and the total-pressure loss coefficient by

$$K_t = \frac{p_{t1} - p_{te}}{\frac{1}{2}\rho \bar{V}_1^2}, \quad (1.2)$$

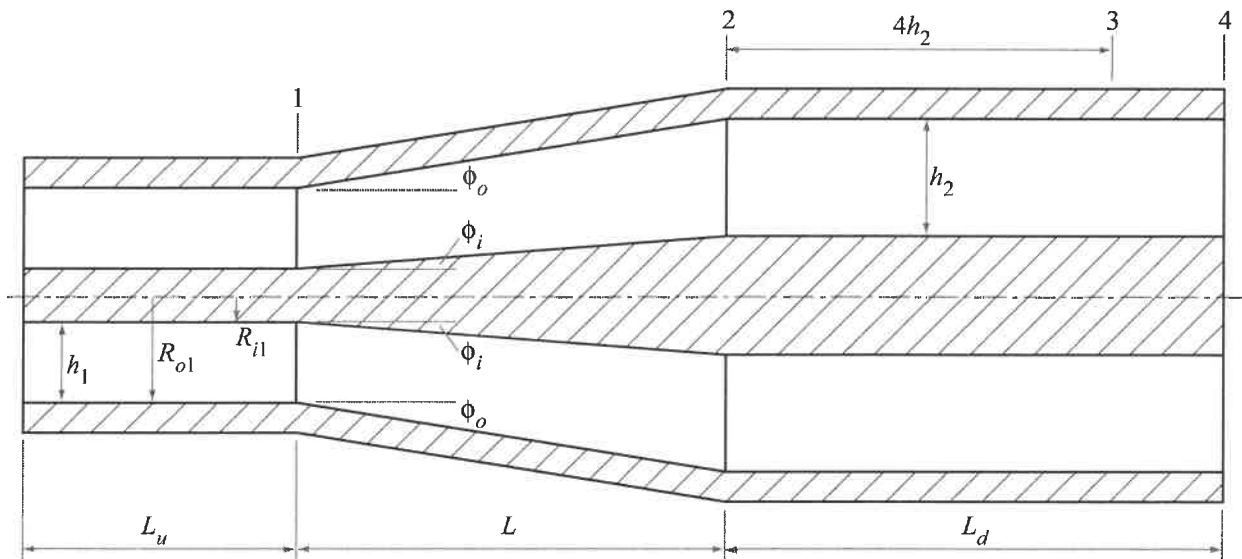
where suffix e is taken as 2 or 3 according to whether the diffuser has free discharge or tailpipe outlet conditions. The static pressure is assumed constant across sections 1 and 2 or 3 and the total pressure is defined as the mass-averaged value given by

$$p_t = p + \alpha(\frac{1}{2}\rho \bar{V}^2), \quad (1.3)$$

where α is the kinetic energy coefficient which relates the mass-averaged kinetic pressure to the product $\frac{1}{2}\rho V^2$, i.e.

$$\alpha = \left(\frac{1}{m} \int_A \frac{1}{2} \rho V^2 dm \right) / \left(\frac{1}{2} \rho \bar{V}^2 \right). \quad (1.4)$$

The geometry of a general annular diffuser and its associated ductwork is shown in section in Sketch 1.1.



Sketch 1.1 Geometry of typical annular diffuser

2. SUMMARY OF DATA PRESENTED AND APPLICABILITY

This Data Item presents information on the performance of some straight-axis, straight-walled diffusers of concentric, circular, annular cross section. The names used in the Item for certain special types are given in Table 8.1 which also includes expressions for the area ratio, A_2/A_1 , in terms of the length ratio, L/h_1 , wall angles ϕ_i and ϕ_o , and the inlet radius ratio, r_1 (Equations (8.1) to (8.7)).

The data given in the Item are derived basically for axi-symmetrical diffusers with smooth corners at entry and with the struts supporting the centre body well outside the diffuser (see Section 4.3.5). The entry flow conditions are basically fully-developed, incompressible annular flow with Reynolds number greater than about 5×10^4 , free from any influence of adjacent duct components. Application of the data for other conditions is discussed in Section 4.3.

The effects of diffuser geometry on the overall flow patterns in the diffusers are discussed in Section 3.

Sections 4.1 and 4.2 discuss the static-pressure recovery coefficient data presented. Data are presented graphically for symmetrical diffusers, parallel core diffusers and general type diffusers (see Table 8.1) with $\phi_i = 5^\circ$. For other types some guidance is given. The area ratio giving maximum C_{pr} for a given length ratio and the length ratio giving maximum C_{pr} for a given area ratio are shown by the C_{pr}^* and C_{pr}^{**} lines respectively. The data are estimated to be generally within ± 0.1 in C_{pr} with the highest uncertainty in values for area ratios greater than 2.

Section 5 shows how a total-pressure loss coefficient can be derived from the static-pressure recovery coefficient. The results are given in equation form only.

3. FLOW CONDITIONS

Figures 1 and 2 show the diffuser geometries in which local separation on a significant scale may be expected to occur in parallel core and symmetrical diffusers (see Table 8.1), based primarily on data from Derivation 4. In the presence (as is usually the case) of radial struts supporting the centre body, the separation in diffusers with geometries in or near the hatched bands is most likely to occur immediately downstream of the struts. As higher area ratios or shorter lengths are used the separated regions increase in volume leading to a lack of symmetry in the outlet flow. For symmetrical diffusers it has been noted in Derivations 4, 6 and 7 that separation occurs only on the outer wall, but for larger angles ($\phi > 10^\circ$) and area ratios ($A_2/A_1 > 6$) than were covered, separation from the inner walls may occur. For other types of diffuser no data were found. For the equiangular (Table 8.1) and general types with small inner wall angles ($\phi_i < 5^\circ$ say) Figure 2 will probably apply approximately. For large values of ϕ_i ($> 15^\circ$), the diffuser entry forms a significant bend and a large rounding radius of about $2h_1$ is advisable to avoid premature separation.

4. STATIC PRESSURE RECOVERY

4.1 Diffusers without Tailpipes

Figure 3 shows C_{pr} for symmetrical annular diffusers (see Table 8.1) with fully-developed entry flow and with free discharge (no tailpipe). Figure 3 is based primarily on data from Derivation 4 reduced as described in Derivation 11. Over the range of values covered ($0 < r_1 < 0.85$), C_{pr} is essentially independent of inlet radius ratio, r_1 , except when the centre-body converges to a point before the end of the diffuser. The maximum area ratio* attainable for a given wall angle if this is not to occur is a function of inlet radius ratio (Equation (8.4))† and is shown on Figure 3. For larger area ratios the diffuser continues beyond the end of the centre body as a plain cone. The true overall area ratio is then given by Equation (8.5)†. No data were found for such cases but as an approximation it is suggested that C_{pr} be taken from Figure 3 at the actual length ratio, L/h_1 , and at an area ratio given by Equation (8.3)†.

Figures 4 to 7 show contours of C_{pr} for parallel core annular diffusers of several inlet radius ratios with fully-developed entry flow and free discharge. For other radius ratios interpolation between these Figures is satisfactory but extrapolation beyond $r_1 = 0.85$ is not recommended. Figures 4 to 7 are based primarily on data from Derivation 4 reduced as described in Derivation 11.

The area ratio for which C_{pr} is a maximum for a given diffuser length ratio and the length ratio for which C_{pr} is a maximum for a given diffuser area ratio are given by the C_{pr}^* and C_{pr}^{**} lines shown on the Figures.

The data found for other types of annular diffuser are insufficient to generalise but some guidance on the pressure recoveries to be expected follows.

Contour plots of C_{pr} developed from an empirical approach in Derivation 11, are given in Figures 8 to 10 for general type diffusers with $\phi_i = 5^\circ$ and for $r_1 = 0, 0.4$, and 0.8 . Values of C_{pr} for other radius ratios may be found by interpolation between these Figures.

For other diffusers with geometries for which the area ratio, A_2/A_1 , and length ratio, L/h_1 , lie in the region around C_{pr}^* an approximate value of C_{pr} may be obtained by reading from Figure 6 at the appropriate values of A_2/A_1 and L/h_1 . The C_{pr}^* line is relatively unaffected² by changes in wall angle and radius ratios in the ranges around $0 < \phi < 15^\circ$ and $0.4 < r_1 < 0.7$, provided that the geometry is

* Equation (8.4) gives the maximum area ratio attainable for $r_1 = 0$ (i.e. a conical diffuser) as 1.0 and Figure 3 therefore does not correspond directly with the conical diffuser data.

† Equations (8.3) to (8.5) are to be found in Table 8.1.

not such as to precipitate separation, *e.g.* a sharp cornered inlet. This approximation is least reliable for geometries where the outer wall angle is small and the inner wall converges rapidly, *e.g.* the parallel casing type.

In the absence of better information for other diffuser types, values of C_{pr} may be obtained by interpolation between suitable curves given in this Item.

4.2 Diffusers with Tailpipes

Pressure recovery contours for parallel core and symmetrical diffusers with tailpipes are shown in Figures 11 to 15 based primarily on data from Derivation 4. The data apply strictly for diffusers with annular tailpipes but the pressure recovery is unlikely to be significantly affected if the centre body is truncated. Downstream of the truncated centre body separated flow may exist for a distance of about $5D_{i2}$ which may have an adverse effect on other components within that distance.

Figures 11 to 15 are derived for tailpipes of length $L_d/h_2 = 4$ approximately but will apply for lengths in the range $4h_2$ to $8h_2$. For longer tailpipes a better approximation is given by

$$C_{pr} = 4f \frac{L_d - 4h_2}{D_{h2}} \left(\frac{A_1}{A_2} \right)^2, \quad (4.1)$$

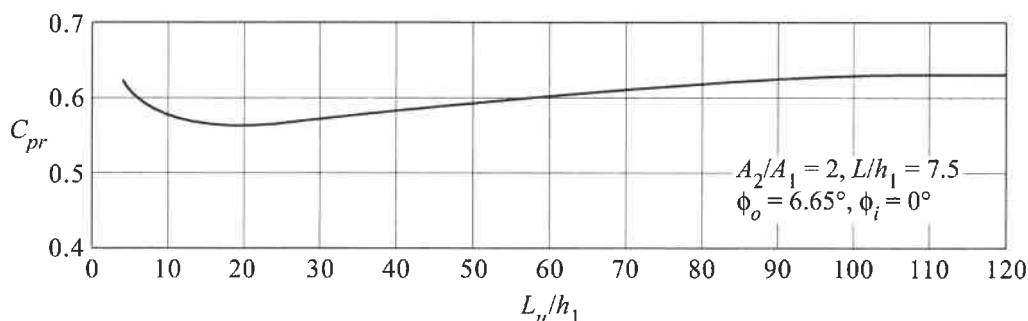
where D_{h2} is the downstream duct hydraulic diameter ($= 2h_2$) and f is the friction factor for the downstream duct, from, for example, ESDU 66027. For shorter tailpipes, interpolation between the value from Figures 11 to 15 with $4h_2$ tailpipe and the value from Figures 3 to 7 without tailpipe gives a good approximation.

4.3 Some Factors Influencing Pressure Recovery

4.3.1 Inlet flow conditions

Naturally-developing flow, diffusers without tailpipes

For naturally-developing flow, C_{pr} for diffusers without tailpipes varies with inlet duct length, L_u/h_1 . Sketch 4.1 shows a typical example of the variation but the precise shape of the curve depends on the diffuser geometry and the conditions at entry to the upstream duct.



Sketch 4.1 Static pressure recovery data from Derivations 6 and 7

Thus to a good approximation the data given in Figures 3 to 10 for fully-developed entry flow may be applied for very short entry lengths provided that the duct entry is profiled so as to avoid local separation or a velocity profile at the diffuser entry which is strongly biased towards one wall. The maximum reduction in C_{pr} between the two extremes of entry length is of the order of 10 per cent for most geometries but increases towards 15 to 20 per cent near C_{pr}^* .

Naturally-developing flow, diffusers with tailpipes

For diffusers with tailpipes the pressure recovery in the tailpipe compensates for variations in inlet conditions where these approximate naturally-developing flow and Figures 11 to 15 may be taken to apply for all inlet lengths, L_u/h_1 .

Other inlet velocity profiles

Inlet velocity profiles which are markedly more asymmetric or more peaky (high ratio of maximum to mean velocity) than the naturally-developing profiles will generally have an adverse, possibly large, effect on the pressure recovery performance of diffusers. However, if the maximum velocity is biased towards the wall on which separation occurs (as noted in Section 3 this is usually the outer wall when that wall diverges) a small improvement in performance may be obtained.

For diffusers with a plain upstream pipe (*i.e.* no centre body) the data in this Item may be expected to apply approximately provided that the upstream end of the diffuser centre body is well profiled so as to avoid local separation and extends a short distance upstream of the minimum area plane.

Swirl

The data in this Item do not apply when a significant swirling component is present in the inlet flow. The separation patterns in the diffuser are altered by swirl in the flow and separation may be completely suppressed or may even occur on the opposite wall to that normally expected (Derivation 5). The interaction of struts with swirling flow is a dominant feature of the flow pattern and it is advisable to place struts as far downstream as possible in the diffuser to minimise adverse effects.

Turbulence

No data were found on the effect of inlet turbulence level on the performance of annular diffusers but it may be expected that small increases up to intensities of about 6 per cent will improve static pressure recovery performance (as is found for conical diffusers) unless accompanied by distortion of the inlet flow. However, an increase in total-pressure loss within the diffuser may be expected.

4.3.2 Inlet Reynolds number and Mach number

The majority of data on which this Data Item is based were obtained for Reynolds numbers around 5×10^4 to 2×10^5 and Mach numbers less than 0.3.

Variations in Reynolds number above $Re = 5 \times 10^4$ are unlikely to cause large changes in C_{pr} but at lower Reynolds number the pressure recovery decreases³.

Data from Derivation 1 show that for small wall angles ($\phi < 6^\circ$), increases in Mach number to as high as 0.7 have little effect on pressure recovery but this value is likely to be reduced as ϕ is increased. Avoidance of sharp corners at the diffuser entry is especially important at high entry Mach numbers.

4.3.3 Junction with inlet duct

In general, sharp corners at the junction of the diffuser and the inlet duct should be avoided. However, for small angles, ϕ_o and ϕ_i up to about 5° , the effect of junction shape may be expected to be small, as for conical diffusers. For large angles, ϕ_o and ϕ_i greater than 10° to 12° , the junction should be well rounded to prevent precipitation of separation. For large angles, where $(\phi_o - \phi_i)$ is small, the inlet region takes on the character of a bend and as such may dominate the flow. An example is given in Derivation 8.

4.3.4 Adjacent components

The effect of upstream components is small provided their outlet flow is axi-symmetric and they are at least $20h_1$ upstream. Components producing asymmetric exit flows tend to reduce diffuser pressure recovery unless at least $30h_1$ upstream and any radial distortion will frequently be amplified by the diffuser. Circumferential distortions, however, tend to mix out.

Components downstream of a diffuser exert little influence unless they are located less than $12h_2$ downstream. Components with uniform resistance close to the diffuser exit such as a flow straightening honeycomb or a tube bank can improve the performance of the diffuser but the component's performance may be adversely affected by asymmetries in the diffuser exit flow.

4.3.5 Centre-body supporting struts

The data given in this Item were derived from tests on experimental diffusers in which interference from centre-body supports was eliminated by placing them well outside the diffuser. Practical diffusers often cannot be constructed in such a manner but the interference can be minimised by using short-chord radial struts (length/chord > 10) of small cross-section (totalling less than about 10 per cent of the annulus area) and placing them in the regions of low pressure gradient towards the end of the diffuser when possible. If long streamwise struts are used which tend to divide the diffuser into segments the flow will be dominated by the effect of the corners between the struts and the walls and the performance will tend towards that of plane-walled diffusers (see, for example, Derivation 10).

5. TOTAL-PRESSURE LOSS

The loss of total pressure in an annular diffuser is strongly influenced by details of geometry and inlet flow which alter the flow pattern at outlet, and the few measured values of total-pressure loss available are insufficient to generalise. However, as shown below, it is possible to evaluate a form of loss coefficient, K_t , which can be used in system total-pressure loss calculations to allow for the presence of the diffuser.

From the definitions of total pressure and total-pressure loss coefficient given in Equations (1.3) and (1.2), a value of K_t applying between the diffuser inlet plane 1 and the exit plane e can be expressed as

$$K_t = \alpha_1 - C_{pr} - \alpha_e \left(\frac{A_1}{A_2} \right)^2. \quad (5.1)$$

The term $\alpha_e (A_1/A_2)^2$ represents the kinetic energy remaining in the flow at the exit plane. If the diffuser or diffuser/tailpipe system discharges into a large space (e.g. the atmosphere) so that this kinetic energy is not utilised in another duct component, the overall loss coefficient between the inlet plane and the large

space is obtained from Equation (5.1) by adding a term equal to $\alpha_e(A_1/A_2)^2$, i.e.

$$K_t = \alpha_1 - C_{pr}. \quad (5.2)$$

For α_1 a value of 1.05, corresponding approximately to fully-developed flow, may be taken. The value of α_e will depend on the diffuser exit conditions and whether a tailpipe is fitted (see Sections 5.1 and 5.2).

By virtue of the definition adopted the effects of the various parameters discussed in Section 4 are opposite to their effects on C_{pr} , i.e. if C_{pr} is reduced K_t is increased, but K_t is also affected by variations in the kinetic energy coefficients α_1 and α_e .

5.1 Diffusers without Tailpipes

For diffusers without tailpipes, α_e in Equation (5.1) equals α_2 . This latter is dependent on the flow patterns in the diffuser and values are not generally available. However, as in this instance the diffuser exhausts to a large space the recoverable kinetic energy at the diffuser exit can be taken as zero and Equation (5.2) may then be applied, which, with $\alpha_1 = 1.05$, gives

$$K_t = 1.05 - C_{pr}, \quad (5.3)$$

where C_{pr} is taken from Figures 3 to 10.

5.2 Diffusers with Tailpipes

Provided that the tailpipe is long enough (at least $4h_2$) for full pressure recovery to occur α_e can be taken as the fully-developed flow value of about 1.05 and from Equation (5.1),

$$K_t = 1.05 \left[1 - \left(\frac{A_1}{A_2} \right)^2 \right] - C_{pr} \quad (5.4)$$

where now C_{pr} is taken directly from Figures 11 to 15 if $L_d/h_2 \approx 4$ or via Equation (4.1) if $L_d/h_2 > 4$.

For L_d/h_2 less than about 4, α_e may be appreciably higher than 1.05 due to distortion of the velocity profile caused by the diffuser and Equation (5.4) will overestimate the total-pressure loss coefficient.

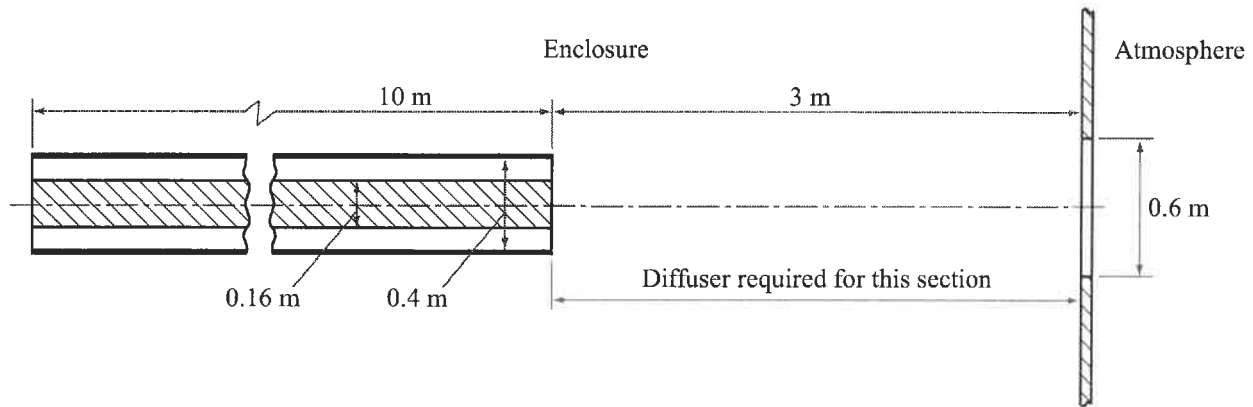
If the tailpipe discharges into a large space rather than to another component then the overall loss coefficient between the diffuser inlet and the large space will be given by Equation (5.2) from which, with $\alpha_1 = 1.05$.

$$K_t = 1.05 - C_{pr}, \quad (5.5)$$

where C_{pr} is taken directly from Figures 11 to 15 or via Equation (4.1) as appropriate.

6. EXAMPLE

An annular diffuser is required to connect an annular duct inside an enclosure to a circular hole in the enclosure wall to discharge to atmosphere, as shown in Sketch 6.1. Both parallel core and symmetrical type diffusers are to be considered to find which will give the higher static-pressure recovery.



Sketch 6.1

The inlet area $A_1 = \frac{\pi}{4}(0.4^2 - 0.16^2) = 0.106 \text{ m}^2$,

the inlet annulus height $h_1 = (0.4 - 0.16)/2 = 0.12 \text{ m}$,

and the inlet radius ratio $r_1 = 0.16/0.4 = 0.4$.

The upstream duct length gives $L_u/h_1 = 10/0.12 = 83.4$. This is somewhat less than the nominal $100h_1$ required for fully-developed entry flow but it can be seen from Sketch 4.1 in Section 4.3.1 that the effect on static-pressure recovery will be small. It will therefore be assumed that no correction for entry conditions is required.

Consider first a parallel core diffuser using the full length.

The exit area $A_2 = \frac{\pi}{4}(0.6^2 - 0.16^2) = 0.263 \text{ m}^2$

and hence the area ratio $A_2/A_1 = 2.48$.

The length ratio $L/h_1 = 3/0.12 = 25$.

For a parallel core diffuser with no tailpipe and with $r_1 = 0.4$, Figure 5 gives the static-pressure recovery coefficient C_{pr} . From Figure 5, for $A_2/A_1 = 2.48$ and $L/h_1 = 25$,

$$C_{pr} = 0.70.$$

For the corresponding symmetrical diffuser, L/h_1 is also 25 but the area ratio is larger since the centre-body now converges at an angle equal to the outer wall angle, given by

$$\tan \phi = (R_{o2} - R_{o1})/L = (0.3 - 0.2)/3 = 0.0333.$$

Equation (8.3) in Table 8.1 conveniently gives the area ratio which is

$$A_2/A_1 = 1 + 2 \times 25 \times 0.0333 = 2.67.$$

This page Amendment A

Equation (8.4) gives the area ratio at which the centre-body will converge to a point which is

$$A/A_1 = 1.4/0.6 = 2.33.$$

The centre-body ends before the end of the diffuser since A is less than A_2 . Equation (8.5) gives the true area ratio but for the purposes of evaluating C_{pr} the value given by Equation (8.3) is used (see Section 4.1). Figure 3 is appropriate to this case and gives, for $L/h_1 = 25$ and $A_2/A_1 = 2.67$, a value of

$$C_{pr} \approx 0.70.$$

In each of these cases it can be seen that for the given A_2/A_1 an optimum diffuser on the C_{pr}^{**} line will be shorter but will have only a marginally improved C_{pr} . However a short tailpipe could then be added which will give some additional improvement.

Consider now diffusers with tailpipes and take the case of a $4h_2$ tailpipe. For a parallel core diffuser, the exit annulus width is

$$h_2 = R_{o2} - R_{i2} = R_{o2} - R_{i1} = 0.3 - 0.08 = 0.22.$$

Thus,
$$4h_2 = 0.88 = (0.88/0.12)h_1 = 7.33 h_1.$$

The length left for the diffuser is therefore,

$$L = (25 - 7.33)h_1 = 17.67 h_1.$$

The area ratio is unchanged at

$$A_2/A_1 = 2.48.$$

Figure 13 is appropriate for this case and from Figure 13 at $L/h_1 = 17.67$ and $A_2/A_1 = 2.48$,

$$C_{pr} \approx 0.71.$$

It can be shown from Equation (8.4) that with the given geometry the centre-body in a symmetrical diffuser will converge to a point before the end of the diffuser for all diffuser lengths.

Thus
$$h_2 = R_{o2} = 0.3 \text{ m and}$$

$$4h_2 = 1.2 \text{ m} = (1.2/0.12)h_1 = 10h_1.$$

The length left for the diffuser is

$$(25 - 10)h_1 = 15h_1.$$

In this case it may be assumed that the tailpipe compensates for the effect of the short centre-body and therefore the actual area ratio can be used for which

$$A_2/A_1 = (\pi/4)(0.6)^2/0.106 = 2.67.$$

Figure 11 is appropriate to this case and for $A_2/A_1 = 2.67$ and $L/h_1 = 15$,

$$C_{pr} = 0.70.$$

Thus it can be seen that the parallel core annular diffuser with a $4h_2$ tailpipe gives marginally the highest pressure recovery coefficient. However, in view of the uncertainty of these values the most practical solution will probably be a parallel core diffuser without tailpipe which will be simpler to manufacture.

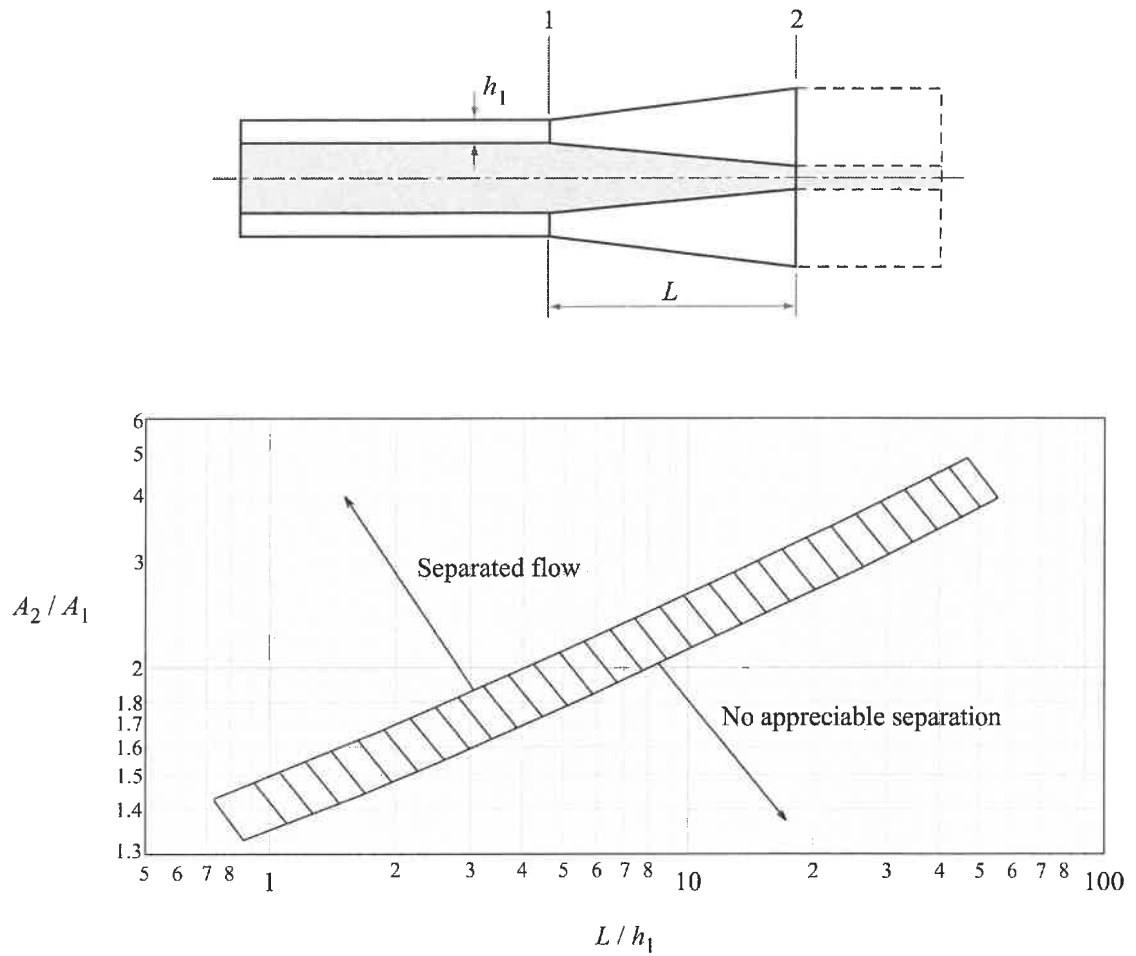
7. DERIVATION

1. NELSON, W.J.
POPP, E.G. Performance characteristics of two 6° and two 12° diffusers at high flow rates. NACA RM L9HO9, 1949.
2. SOVRAN, G.
KLOMP, E.D. Experimentally determined optimum geometries for rectilinear diffusers with rectangular, conical or annular cross-section. Proc. Fluid Mech. Int. Flow Symp., General Motors, Michigan, 1965, pp. 270-319, published Elsevier, New York, 1967.
3. DRISCOLL, F.B. Incompressible flow in annular diffusers with cylindrical centre-bodies. M.S.Thesis, Purdue Univ., 1967.
4. HOWARD, J.H.G
HENSELER, H.J
THORNTON-TRUMP, A.B. Performance and flow regimes for annular diffusers. Am. Soc. mech. Engrs, Paper No. 67-WA/FE-21, 1967.
5. HOADLEY, D. Boundary layer development in an annular diffuser. Paper 4, Symp. Internal Flows, Univ. Salford, April 1971; Proc. pp. A19-A31, 1971.
6. STEVENS, S.J.
WILLIAMS, G.J. Measurements of the overall performance and boundary layer growth in an annular diffuser. Paper 3, Symp. Internal Flows, Univ. Salford, April 1971; Proc. pp. A9-A18, 1971.
7. WILLIAMS, G.J. The influence of inlet conditions on the boundary layer growth and overall performance of annular diffusers. Ph.D. Thesis, Univ. Technology, Loughborough, 1972.
8. STEVENS, S.J.
FRY, P. Measurements of boundary layer growth in annular diffusers. *J. Aircr.*, Vol. 10, No. 2, pp. 73-80, 1973.
9. – Performance of conical diffusers in incompressible flow. Engng Sciences ESDU 73024, 1973.
10. – Performance in incompressible flow of plane-walled diffusers with single-plane expansion. Engng Sciences ESDU 74015, 1974.
11. FREEMAN, B.C. The evaluation of annular diffuser data. ESDU Memor. No. 16, Engng Sciences Data Unit, 1975.

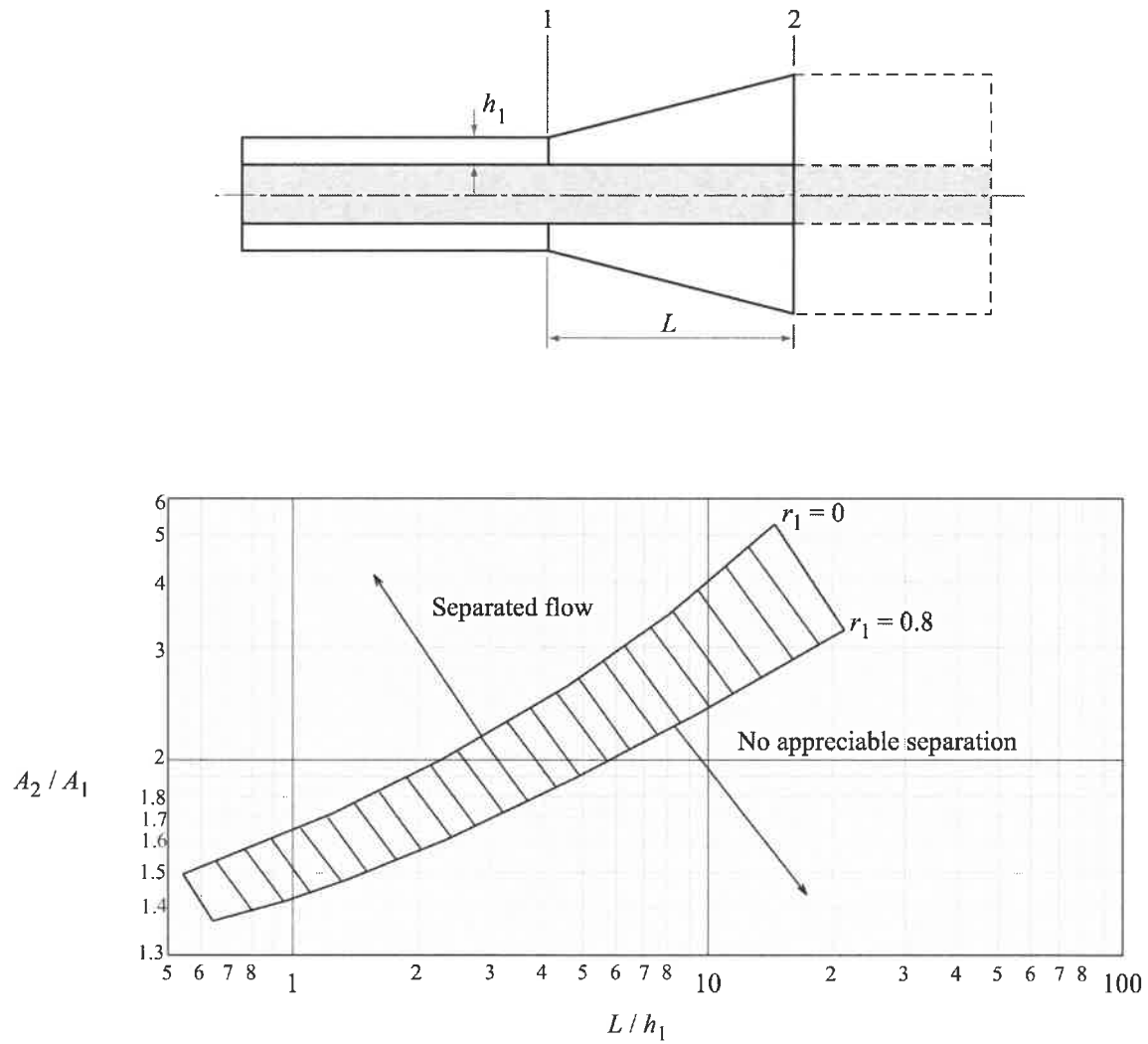
8. TABLES

TABLE 8.1 Special Cases of Annular Diffusers

Type	Sketch	Area Ratio
General $(\phi_o \text{ positive, } \phi_i \text{ can be negative})$		$\frac{A_2}{A_1} = 1 + \frac{2}{1+r_1} \frac{L}{h_1} (\tan \phi_o - r_1 \tan \phi_i) + \frac{1-r_1}{1+r_1} \left(\frac{L}{h_1} \right)^2 (\tan^2 \phi_o - \tan^2 \phi_i) \quad (8.1)$
Equiangular $(\phi_i = \phi_o)$		$\frac{A_2}{A_1} = 1 + 2 \frac{1-r_1}{1+r_1} \frac{L}{h_1} \tan \phi \quad (8.2)$
Symmetrical (about flow passage centre line) $(\phi_i = -\phi_o)$		$\frac{A_2}{A_1} = 1 + 2 \frac{L}{h_1} \tan \phi_o \quad (8.3)$ <p>The centre core converges to a point when</p> $\frac{A}{A_1} = \frac{1+r_1}{1-r_1} \quad \text{and} \quad \frac{x}{h_1} = \frac{r_1}{1-r_1} \frac{1}{\tan \phi_o} \quad (8.4)$ <p>and for longer diffusers the overall area ratio is</p> $\frac{A_2}{A_1} = \frac{1-r_1}{1+r_1} \left[\frac{1}{1-r_1} + \frac{L}{h_1} \tan \phi_o \right]^2 \quad (8.5)$
Parallel core $(\phi_i = 0)$		$\frac{A_2}{A_1} = 1 + \frac{2}{1+r_1} \frac{L}{h_1} \tan \phi_o + \frac{1-r_1}{1+r_1} \left(\frac{L}{h_1} \tan \phi_o \right)^2 \quad (8.6)$
Parallel casing $(\phi_o = 0)$		$\frac{A_2}{A_1} = 1 - \frac{2r_1}{1+r_1} \frac{L}{h_1} \tan \phi_i - \frac{1-r_1}{1+r_1} \left(\frac{L}{h_1} \tan \phi_i \right)^2 \quad (8.7)$ <p>[Note that ϕ_i is negative]</p>



**FIGURE 1 GEOMETRY FOR ONSET OF SIGNIFICANT LOCAL SEPARATION
IN SYMMETRICAL ANNULAR DIFFUSERS**



**FIGURE 2 GEOMETRY FOR ONSET OF SIGNIFICANT LOCAL SEPERATION
IN PARALLEL CORE ANNULAR DIFFUSERS**

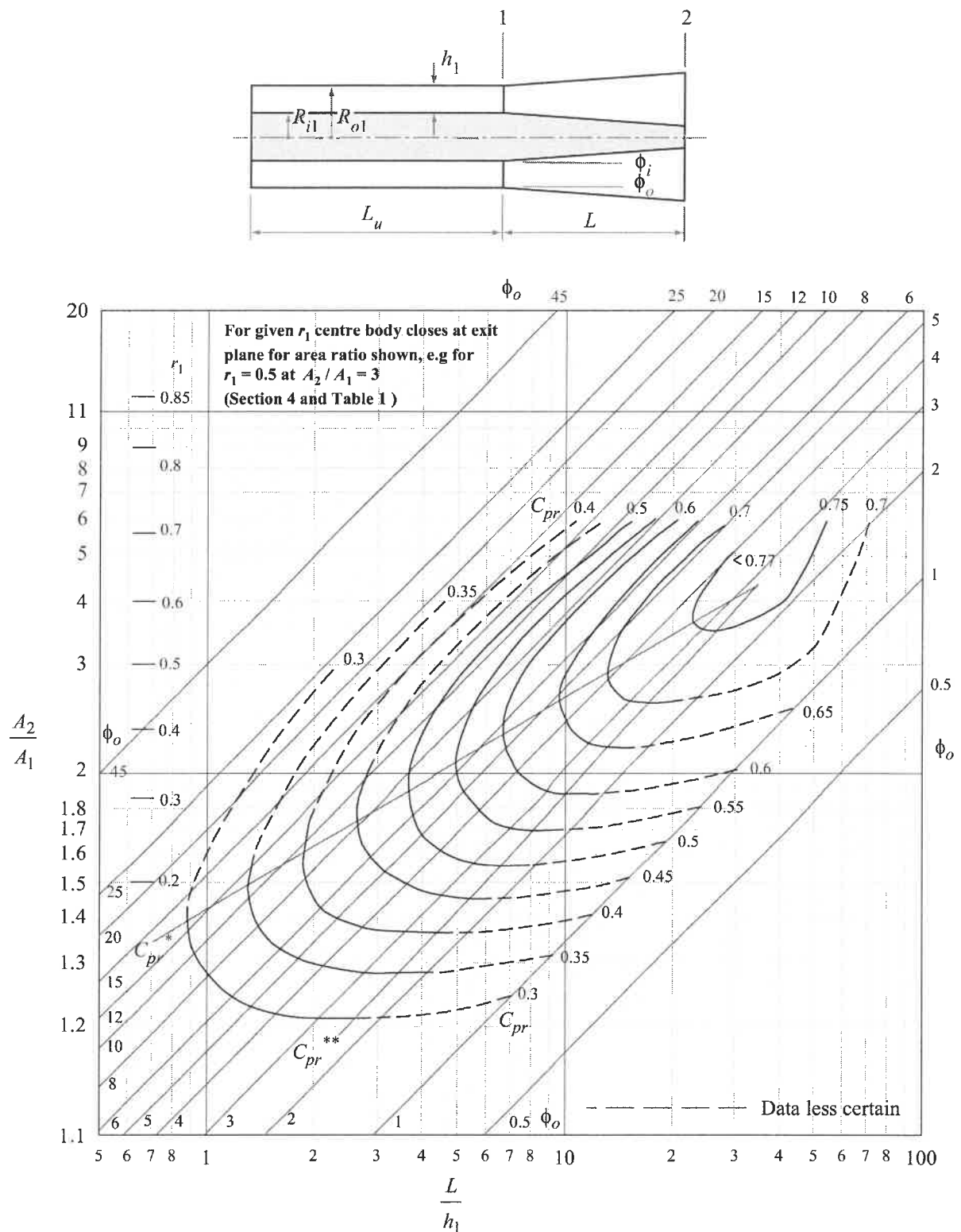


FIGURE 3 STATIC-PRESSURE RECOVERY COEFFICIENT, SYMMETRICAL ANNULAR DIFFUSERS

WITHOUT TAILPIPES, $\frac{L_d}{h_2} = 0$, FULLY-DEVELOPED ENTRY FLOW, $\frac{L_u}{h_1} \geq 100$

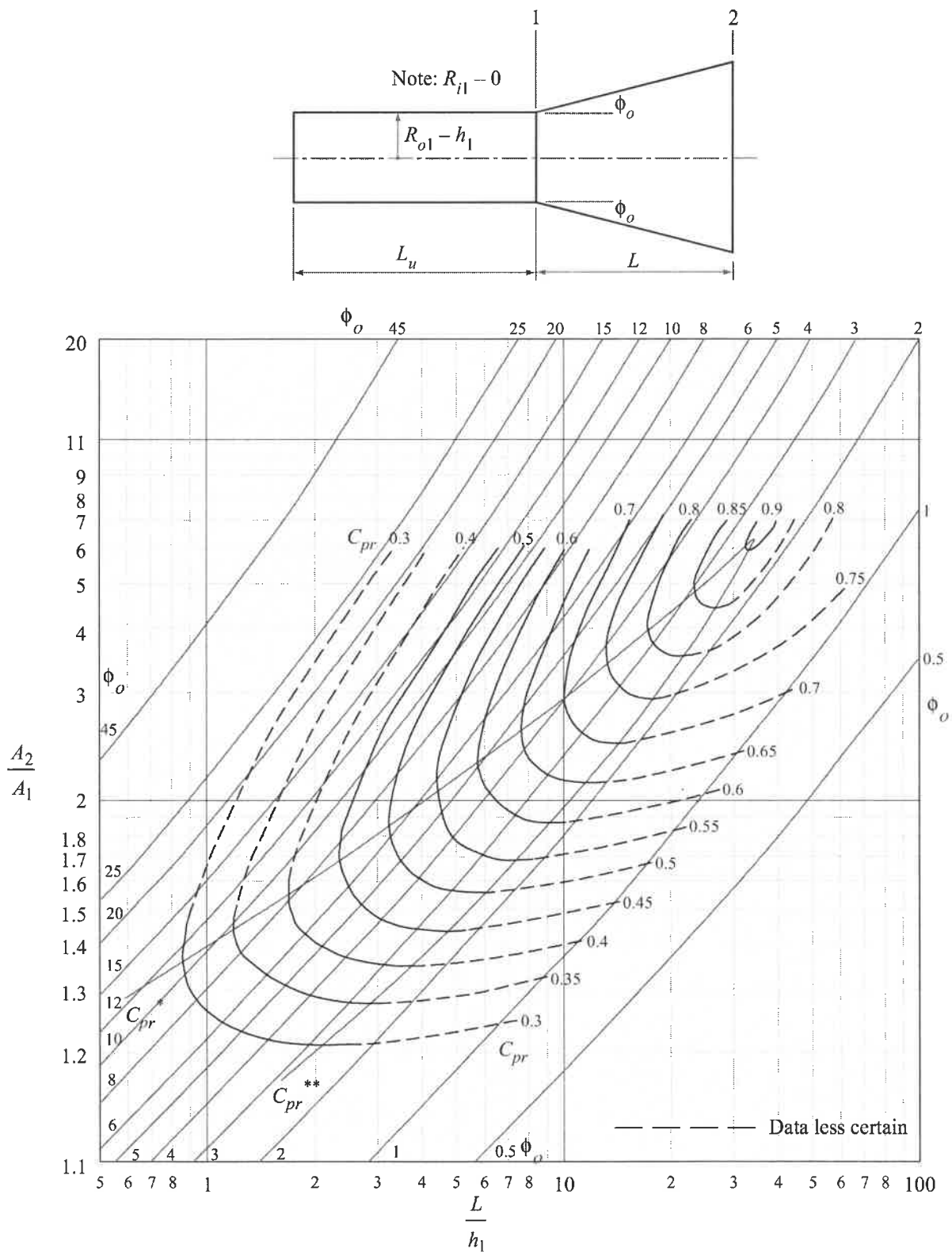


FIGURE 4 STATIC-PRESSURE RECOVERY COEFFICIENT, PARALLEL CORE ANNULAR DIFFUSERS,

$r_1 = 0$, WITHOUT TAILPIPES, $\frac{L_d}{h_2} = 0$, FULLY-DEVELOPED ENTRY FLOW, $\frac{L_u}{h_1} \geq 100$.

(EQUIVALENT TO CONICAL DIFFUSERS, DATA FROM ESDU 73024)

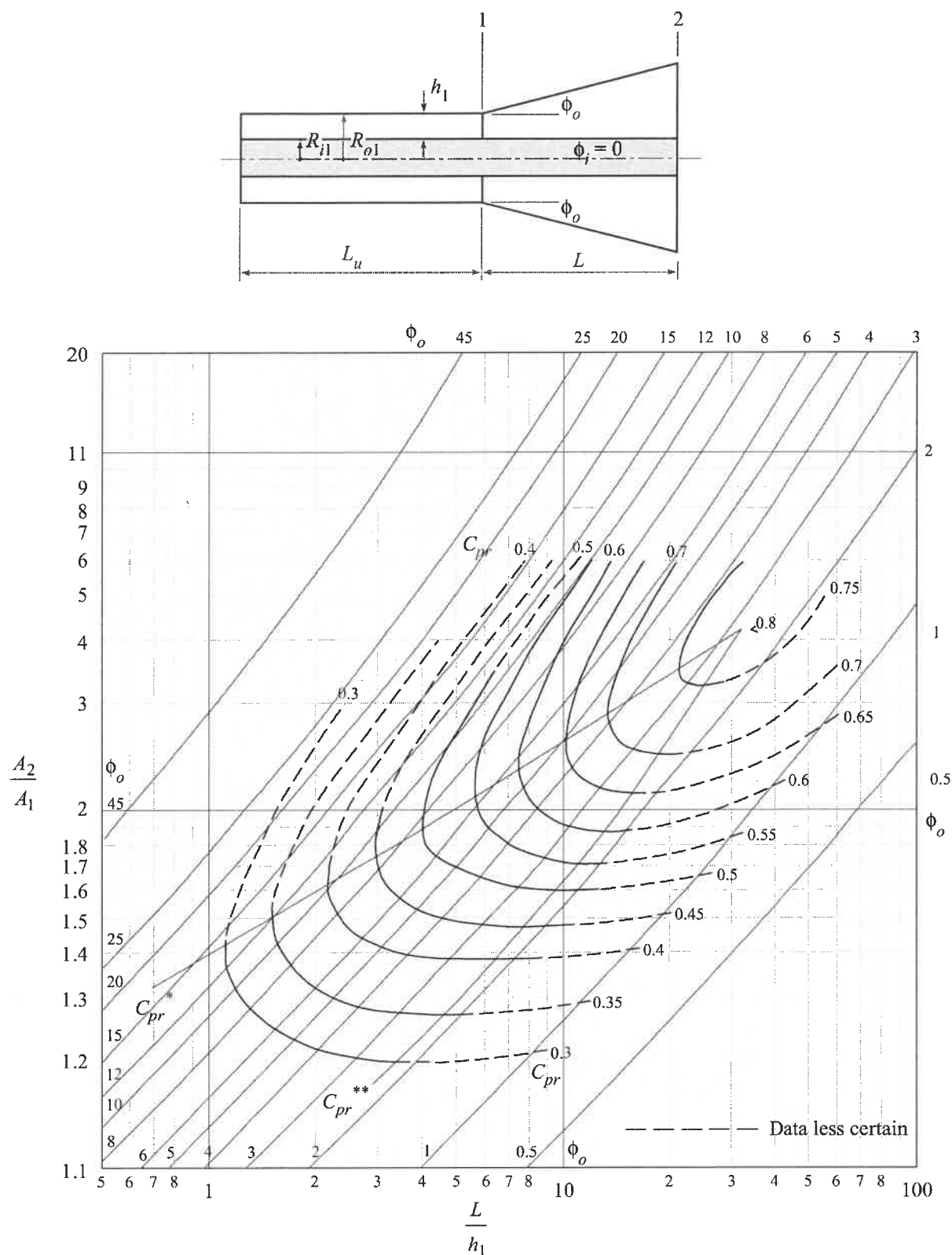


FIGURE 5 STATIC-PRESSURE RECOVERY COEFFICIENT, PARALLEL CORE ANNULAR DIFFUSERS,

$$r_1 = 0.4, \text{ WITHOUT TAILPIPES, } \frac{L_d}{h_2} = 0, \text{ FULLY-DEVELOPED ENTRY FLOW, } \frac{L_u}{h_1} \geq 100$$

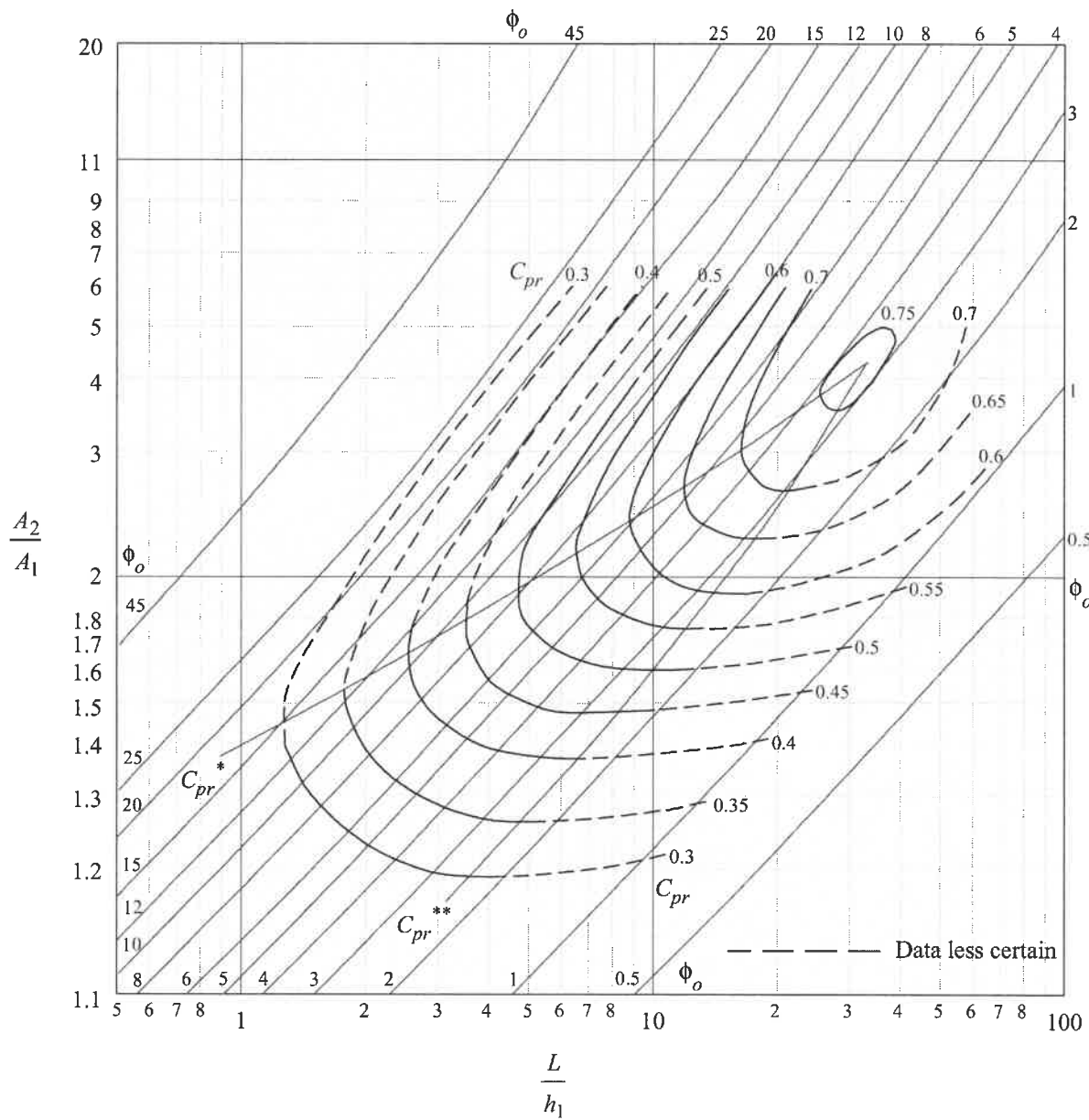
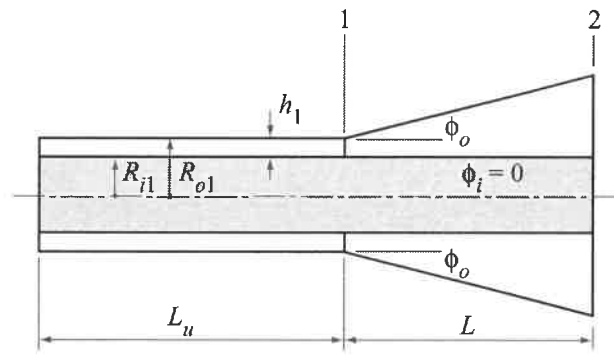


FIGURE 6 STATIC-PRESSURE RECOVERY COEFFICIENT, PARALLEL CORE ANNULAR DIFFUSERS,

$r_1 = 0.6$, WITHOUT TAILPIPES, $\frac{L_d}{h_2} = 0$, FULLY-DEVELOPED ENTRY FLOW, $\frac{L_u}{h_1} \geq 100$

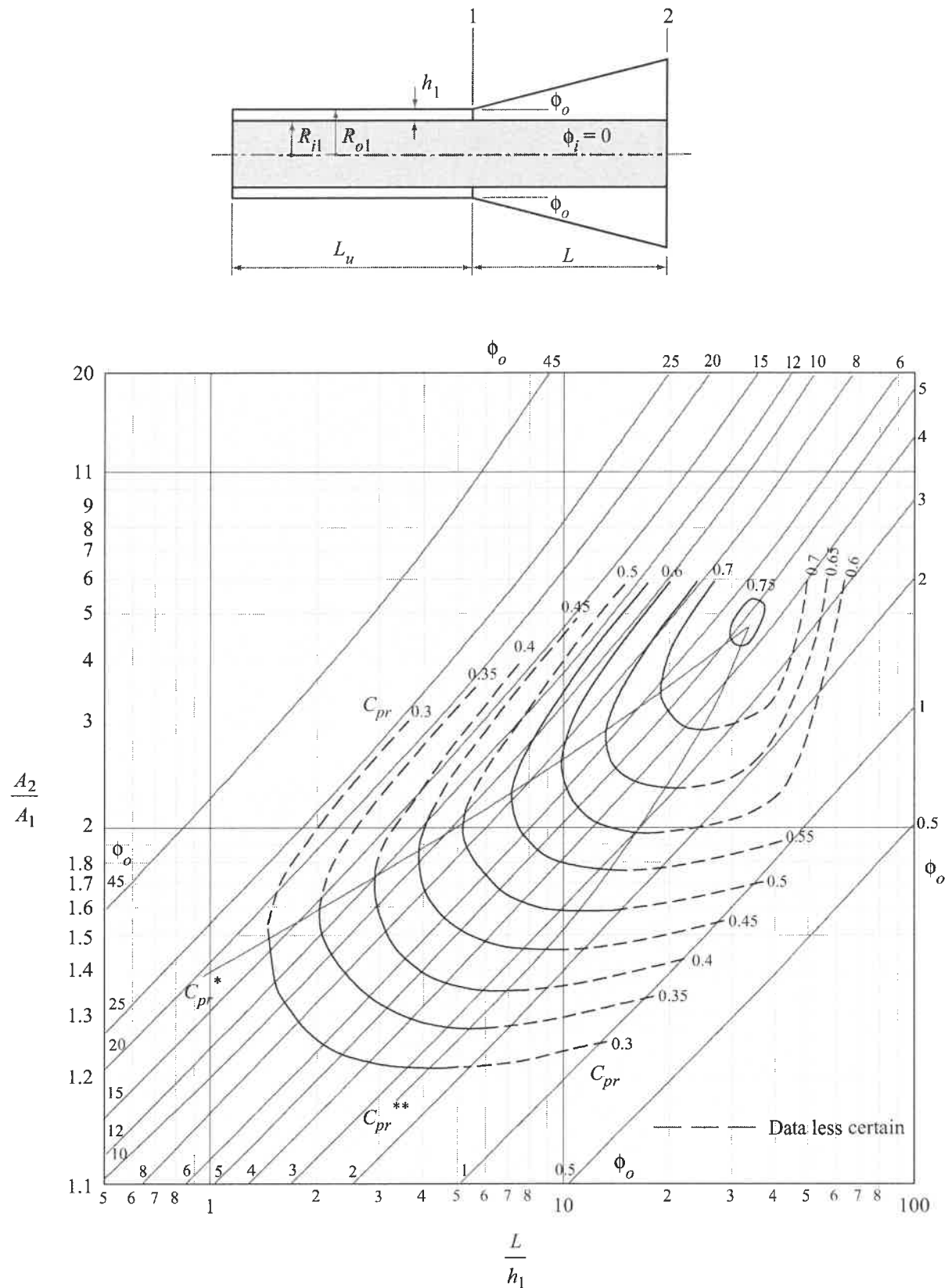


FIGURE 7 STATIC-PRESSURE RECOVERY COEFFICIENT, PARALLEL CORE ANNULAR DIFFUSERS,

$r_1 = 0.8$, WITHOUT TAILPIPES, $\frac{L_d}{h_2} = 0$, FULLY-DEVELOPED ENTRY FLOW $\frac{L_u}{h_1} \geq 100$

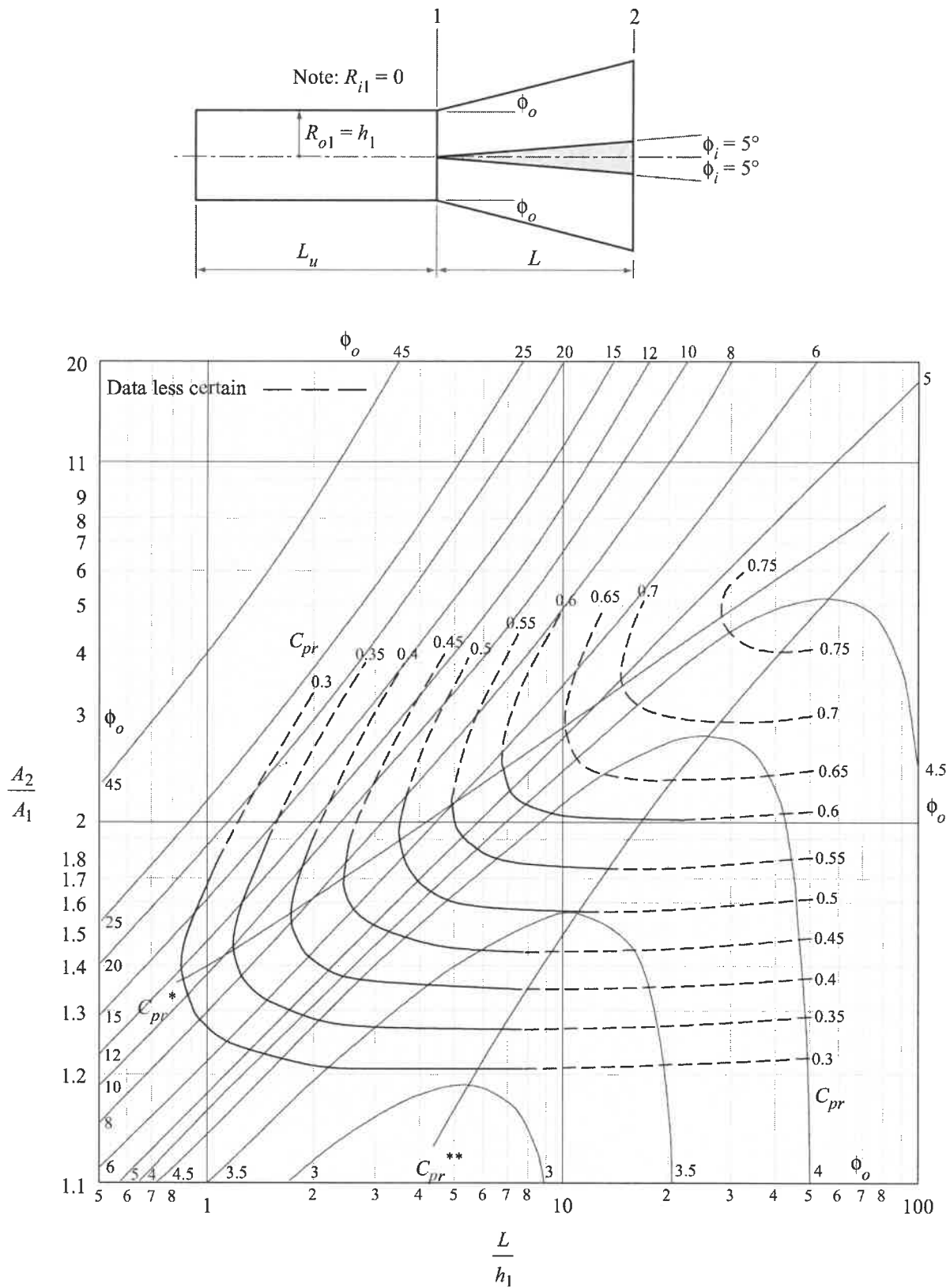


FIGURE 8 STATIC-PRESSURE RECOVERY COEFFICIENT, ANNULAR DIFFUSERS WITH $\phi_i = 5^\circ$ AND

$r_1 = 0$, WITHOUT TAILPIPES, $\frac{L_d}{h_2} = 0$, FULLY-DEVELOPED ENTRY FLOW $\frac{L_u}{h_1} \geq 100$

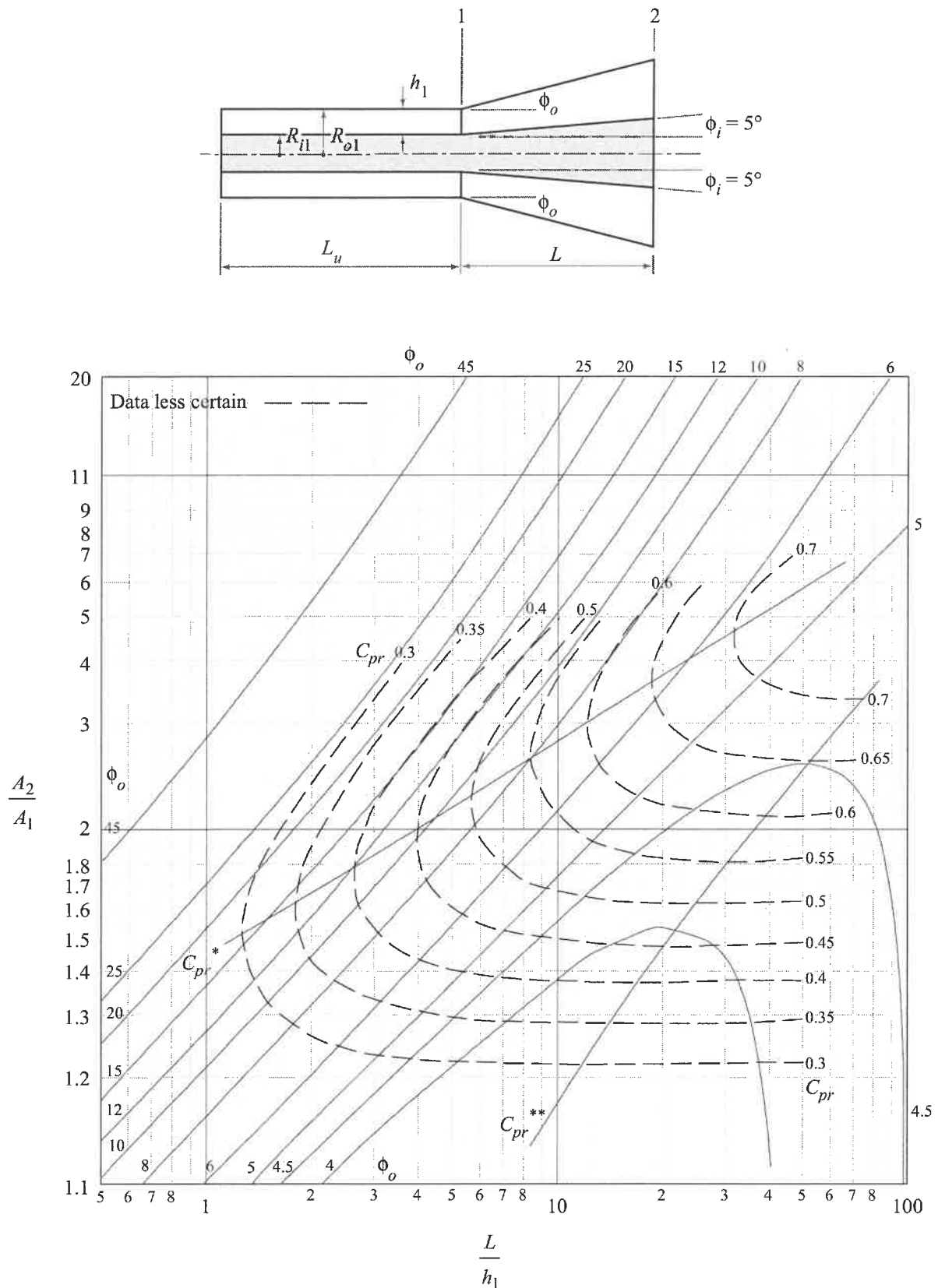


FIGURE 9 STATIC-PRESSURE RECOVERY COEFFICIENT, ANNULAR DIFFUSERS WITH $\phi_1 = 5^\circ$ AND

$r_1 = 0.4$, WITHOUT TAILPIPES, $\frac{L_d}{h_2} = 0$, FULLY-DEVELOPED ENTRY FLOW $\frac{L_u}{h_1} \geq 100$

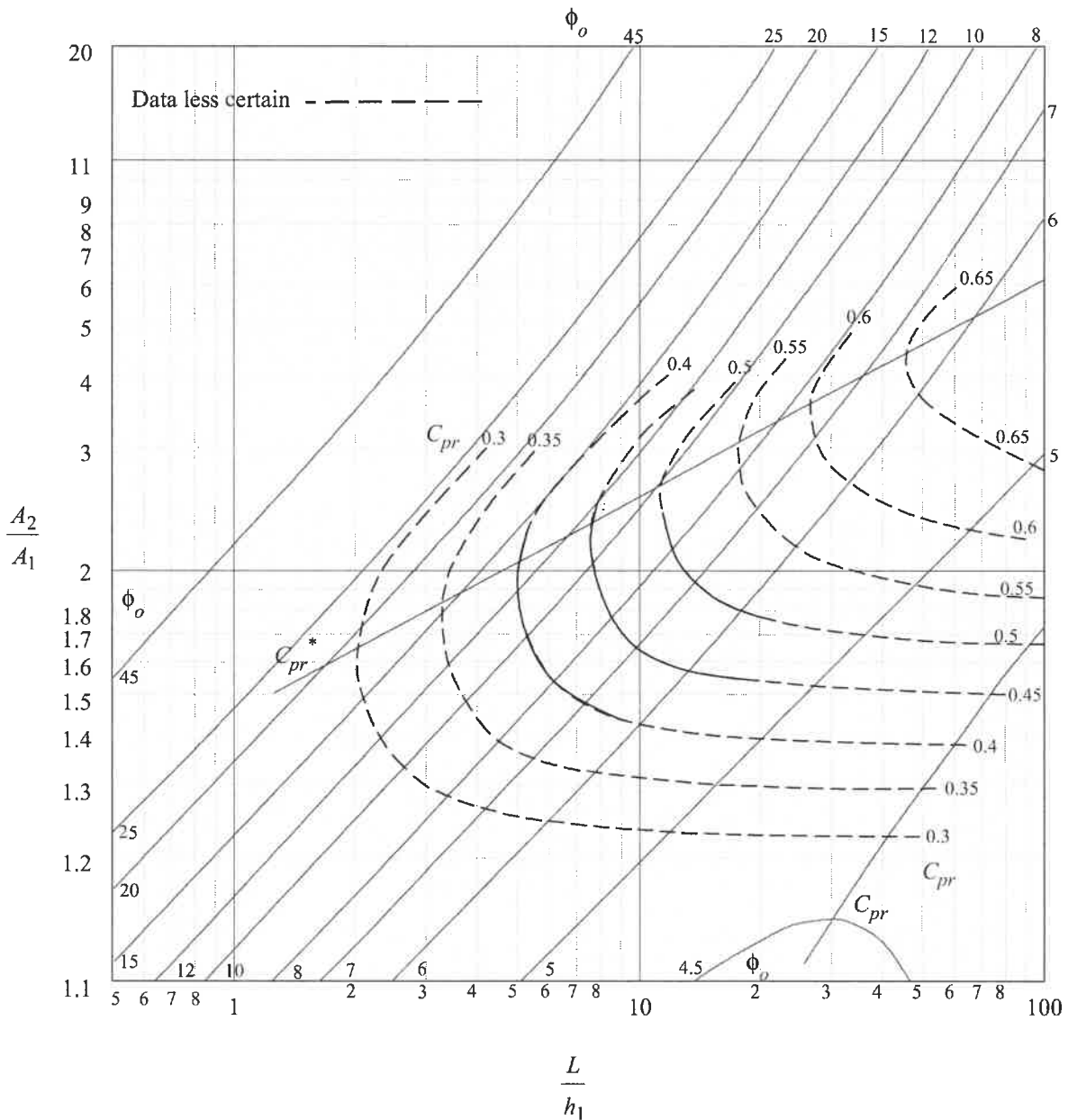
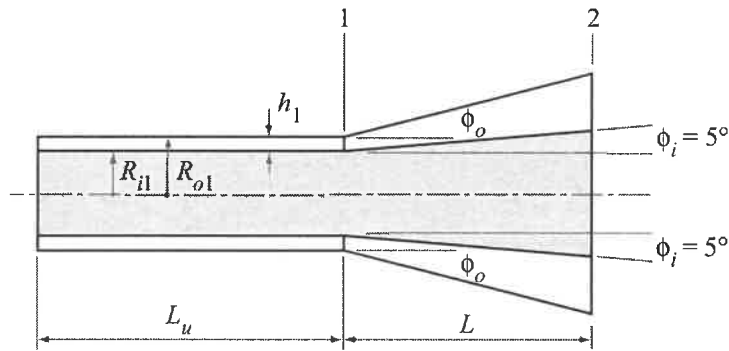


FIGURE 10 STATIC-PRESSURE RECOVERY COEFFICIENT, ANNULAR DIFFUSERS WITH $\phi_1 = 5^\circ$

AND $r_1 = 0.8$, WITHOUT TAILPIPES, $\frac{L_d}{h_2} = 0$, FULLY-DEVELOPED ENTRY FLOW $\frac{L_u}{h_1} \geq 100$

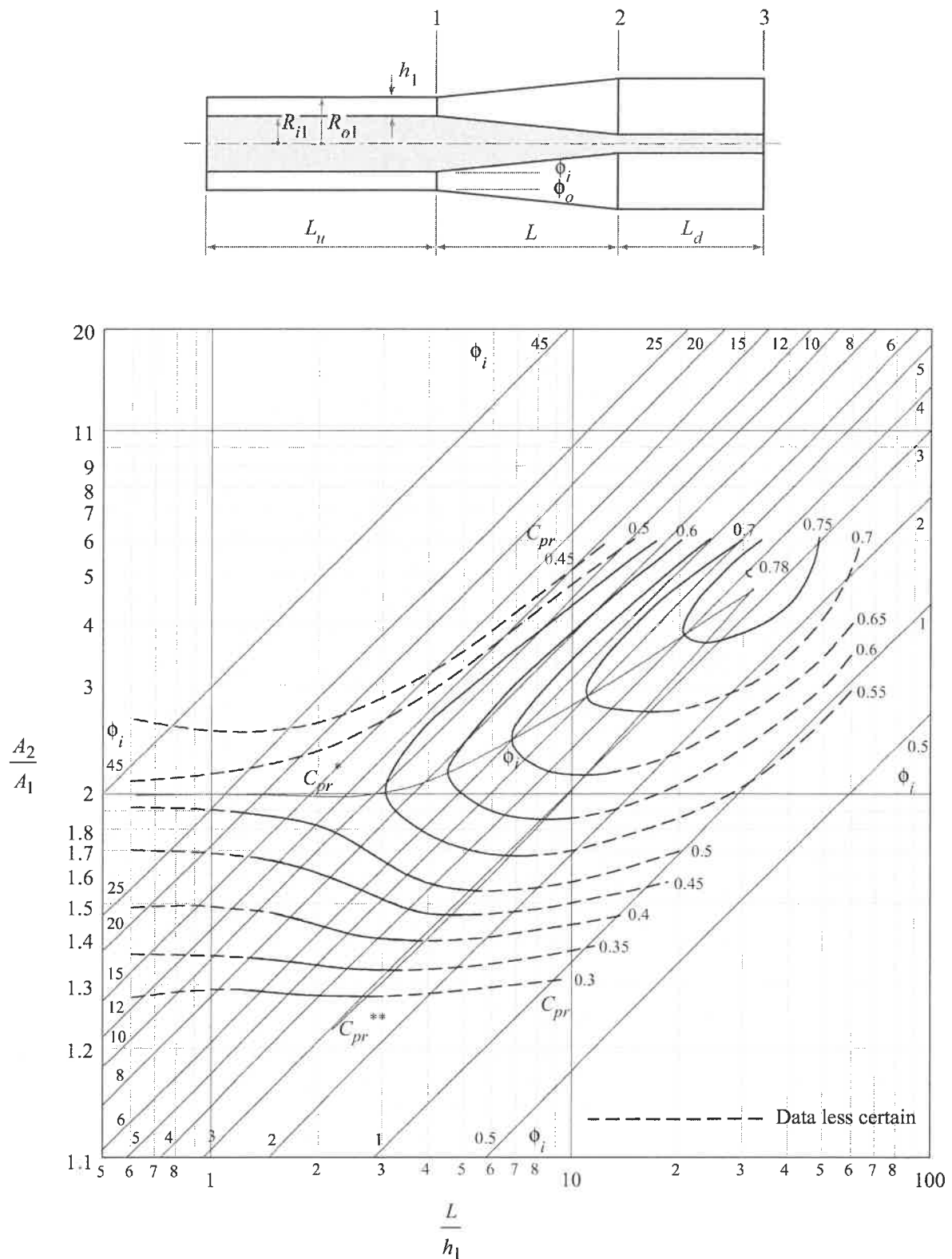


FIGURE 11 STATIC-PRESSURE RECOVERY COEFFICIENT, SYMMETRICAL

ANNULAR DIFFUSERS WITH TAILPIPES, $\frac{L_d}{h_2} = 4$

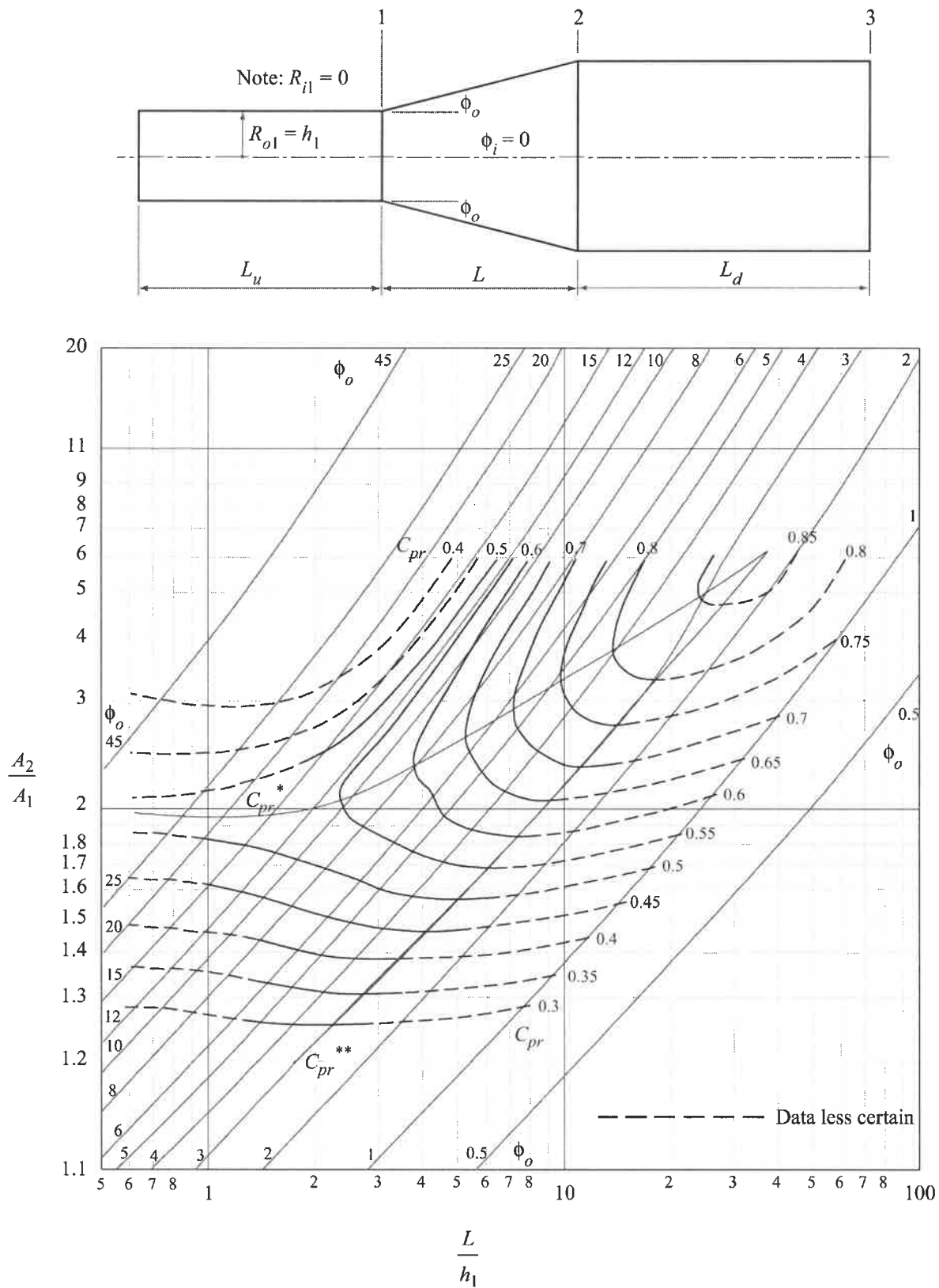


FIGURE 12 STATIC-PRESSURE RECOVERY COEFFICIENT, PARALLEL CORE ANNULAR DIFFUSERS,

$$r_1 = 0, \text{ WITH TAILPIPES, } \frac{L_d}{h_2} = 4, \text{ (EQUIVALENT TO CONICAL DIFFUSER.)}$$

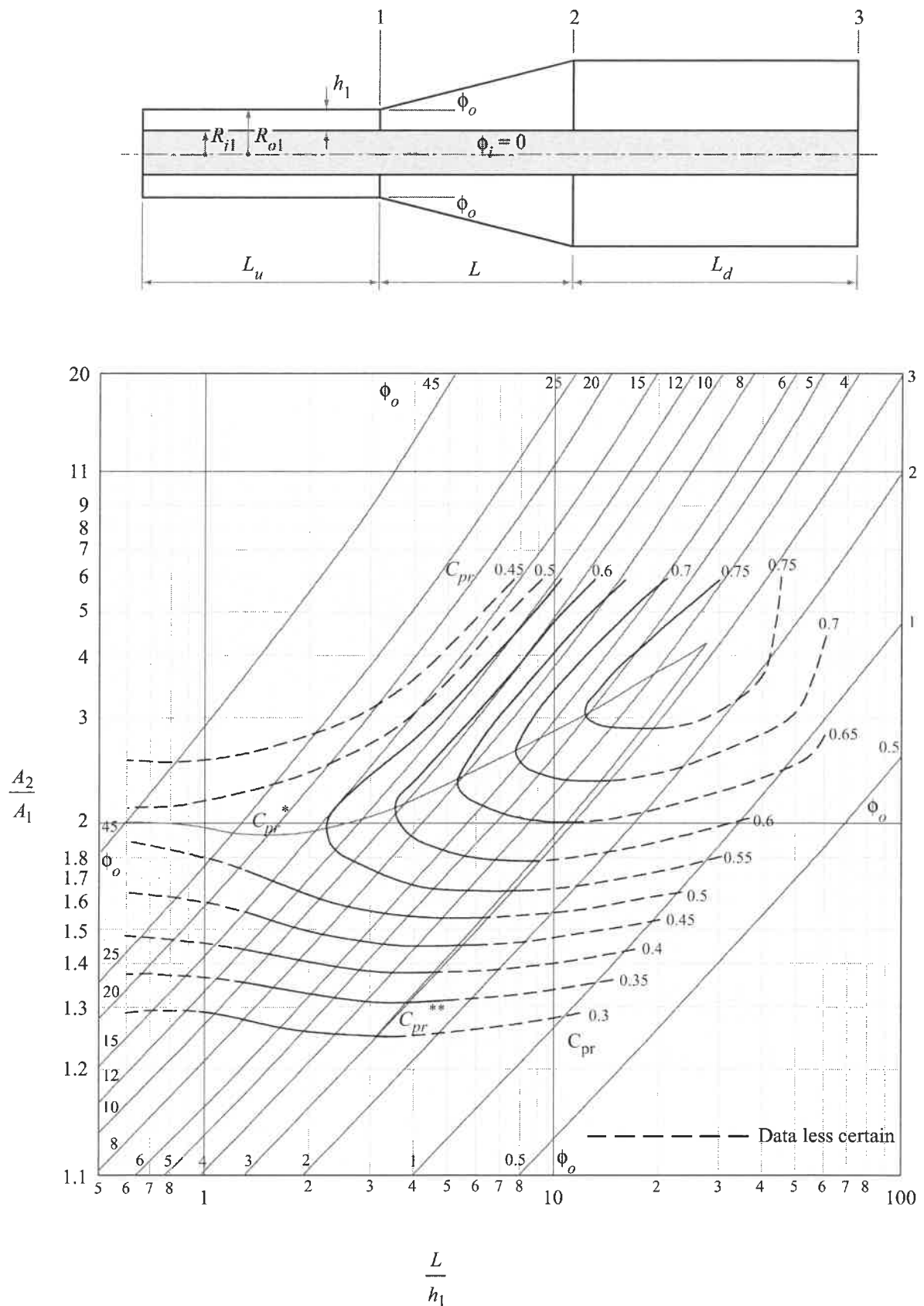


FIGURE 13 STATIC-PRESSURE RECOVERY COEFFICIENT, PARALLEL CORE ANNULAR DIFFUSERS,

$$r_1 = 0.4, \text{ WITH TAILPIPES, } \frac{L_d}{h_2} = 4,$$

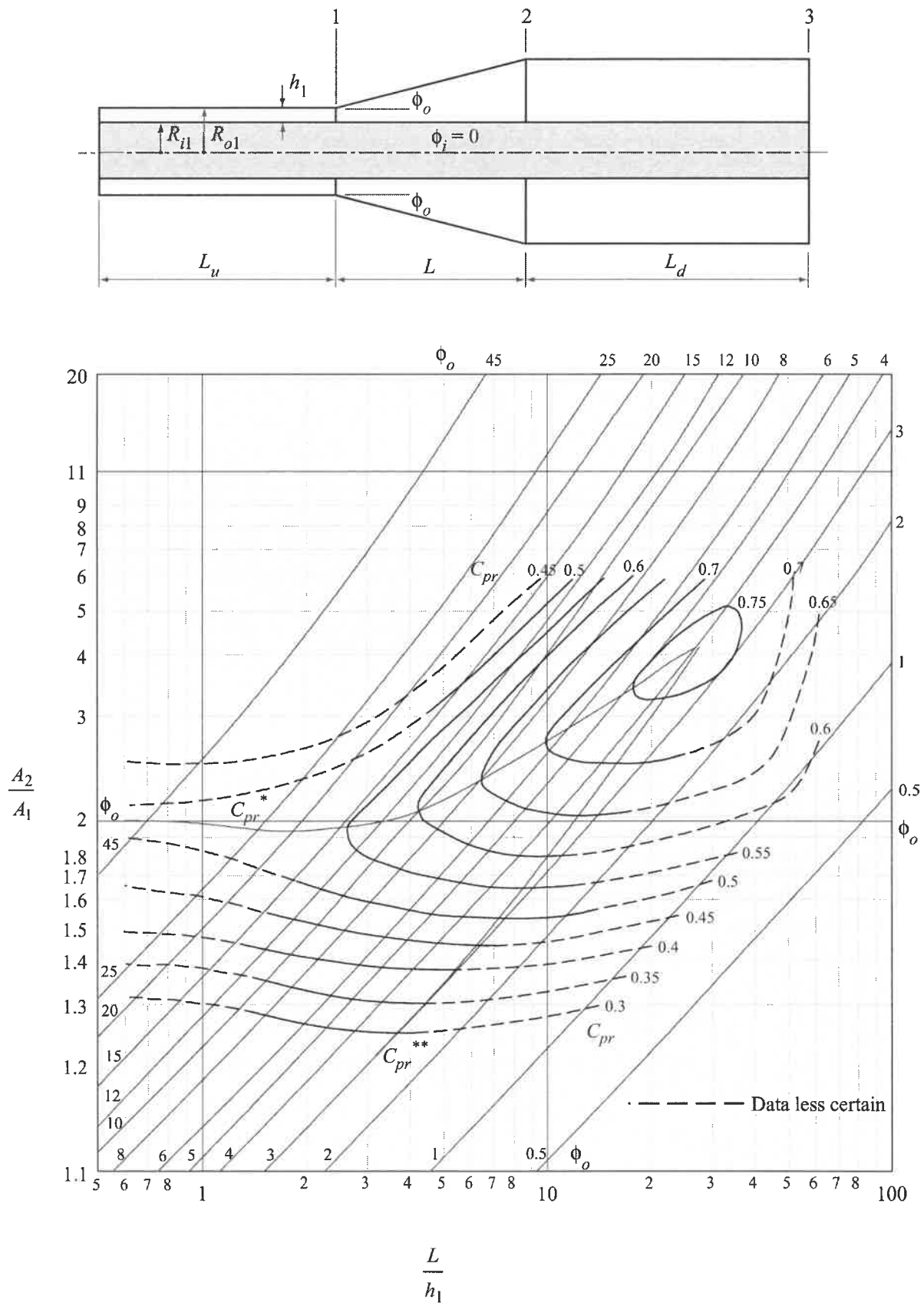


FIGURE 14 STATIC-PRESSURE RECOVERY COEFFICIENT, PARALLEL CORE ANNULAR DIFFUSERS,

$$r_1 = 0.6, \text{ WITH TAILPIPES, } \frac{L_d}{h_2} = 4,$$

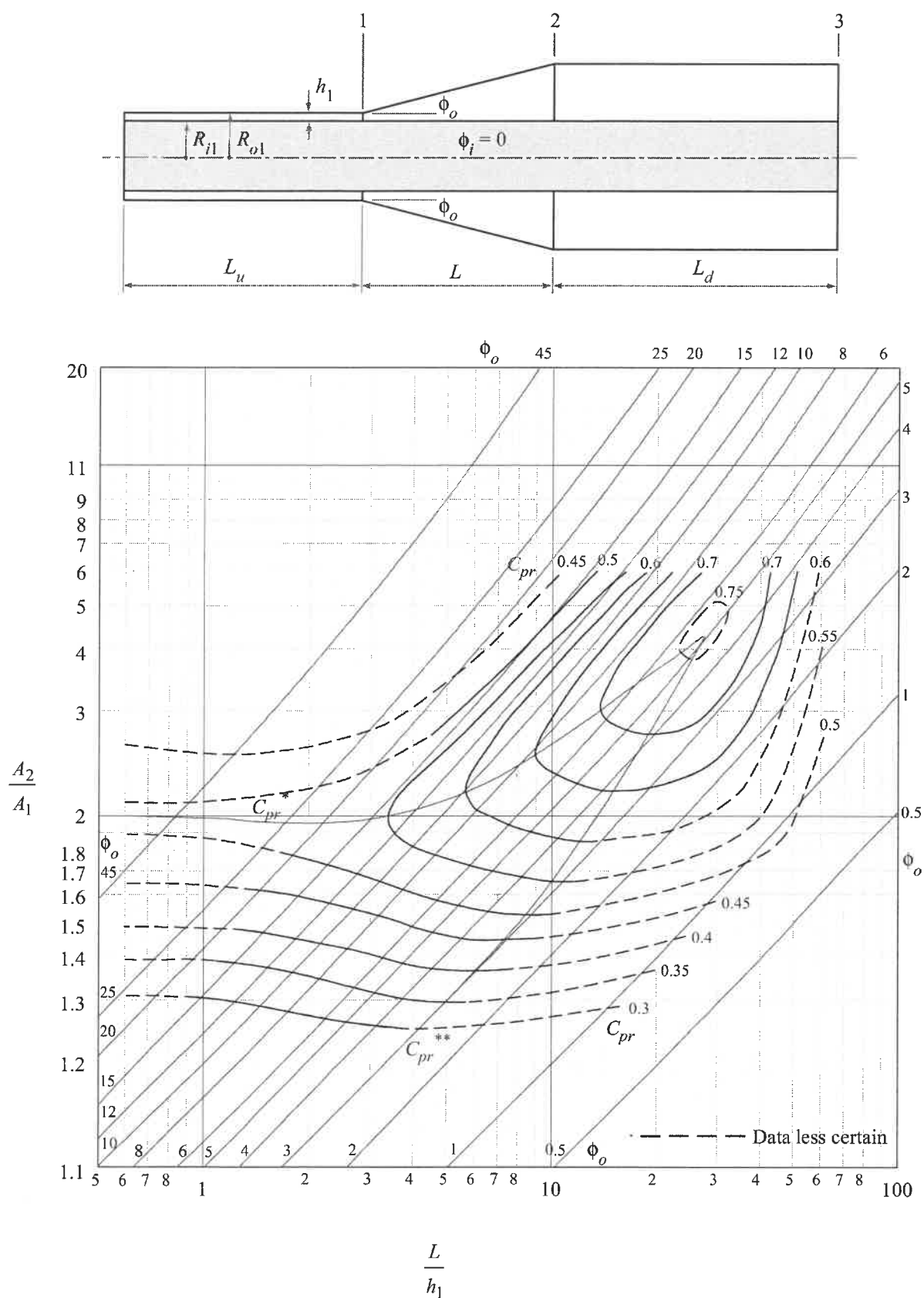


FIGURE 15 STATIC-PRESSURE RECOVERY COEFFICIENT, PARALLEL CORE ANNULAR DIFFUSERS,

$$r_1 = 0.8, \text{ WITH TAILPIPES, } \frac{L_d}{h_2} = 4,$$

